ISSN 2004-2965 Energy Proceedings, Vol. 22, 2021

International Conference on Applied Energy 2021
Nov. 29 - Dec. 5, 2021, Thailand/Virtual
Paper ID: 749

Variable Refrigeration Flow System Simultaneous Fault Diagnosis Based on Deep Convolutional Network

Zhenxin Zhou[1], Huanxin Chen [1*]

Department of Refrigerant and Cryogenics Engineering, School of Energy and Power Engineering, Huazhong University of Science and Technology, Wuhan 430074, China

ABSTRACT

The potential for saving on energy related cost with timely and accurate Fault Detection and Diagnosis (FDD) in the air-conditioning system which is as one of the major energy consumer in buildings has been estimated to huge. In recent years, the research on fault diagnosis of air-conditioning systems has mostly focused on single fault or multiple faults. While, there is less research on simultaneous faults because of the complexity of simultaneous faults. This paper proposes a diagnosis method based on deep convolutional neural network, which can effectively diagnose the common two simultaneous faults and three simultaneous faults in variable flow systems. The results show that this method can effectively isolate faults in the case of multiple faults and multiple-simultaneous faults. The diagnostic accuracy is over 98%, and the Hamming loss value is lower 1. 5%.

Keywords: deep convolutional neural network, Variable refrigerant flow system, simultaneous faults, Fault diagnosis, Artificial intelligence

1. INTRODUCTION

The energy consumed by the buildings and buildings construction sectors is constantly rising, accounting for 36% of the final global energy in 2018[1]. The air-conditioning system is one of the primary energy consumers in buildings[2], exceeding 50%[3]. Especially in China, as the requirements for building indoor thermal comfort continue to increase, it accounts for more than 30% of the total residential electricity consumption[4]. According to a survey of UK buildings, using automatic fault detection and diagnosis (AFDD) technology to diagnose faults in the early stage, we can reduce energy waste caused by the HVAC&R system faults to less than 15%. Without a diagnosis, the energy waste will reach 25-50%[5]. Therefore, establishing AFDD models to reduce energy consumption in air-conditioning systems has become a research hotspot in the past two decades[6, 7].

The FDD method in the HVAC system can usually be classified into three approaches[8]: model-based, knowledge-based, and data-based. In this classification, 62% of the publications employ process history (data-driven) models since the data-driven method is more suitable to modern engineering systems with large-scale domains[5]. In addition, using data-driven methods, excellent results have been achieved in the fault diagnosis of sensors[9, 10], valves fault[11], refrigerant undercharge/upcharge[12], and condenser/evaporator fouling[13, 14] of the air conditioning system. Therefore, it's a feasible research direction to use data-driven methods for air-conditioning system fault diagnosis.

The fault diagnosis of the air-conditioning system started with a single fault[12], and then gradually extended to multiple faults[15]. The predecessors made many contributions to the fault diagnosis of the air-conditioning system. However, due to the complexity of simultaneous faults, the diagnosis becomes more difficult, and there is less research on it. Wu et.al[16] proposed a hybrid data-driven diagnosis model for air handling units simultaneous faults. Asgari et.al[17] proposed a data-driven approach to simultaneous fault detection and diagnosis in data centers. None of these research objects involve VRF systems. But in actual situations, simultaneous faults are inevitable in VRF system. Carrying out simultaneous fault diagnosis for VRF system has realistic background and practical significance.

2. METHOD

2.1 Convolutional Neural Networks

Convolutional neural network (CNN) consists of three layers, convolutional layers, pooling layers, and a fully-connected layer. And the convolutional layers have convolutional filters and a nonlinear activation function. A CNN architecture as following:

Selection and peer-review under responsibility of the scientific committee of the 13th Int. Conf. on Applied Energy (ICAE2021).

Firstly, before activation function, the convolutional filters make new feature maps u through convolution operation with input data x in the l_{th} layer:

$$u_{ij}^{l} = \sum_{a=1}^{A}\sum_{b=1}^{B} w_{ab}^{l} x_{i+a-1\ \ j+b-1}^{l-1} + b_{ij}^{l} \tag{1}$$

where A is the height of a convolutional filter, B is the width of a convolutional filter, w is the weight parameter of convolutional filters and b is a bias.

After the convolution operation, a nonlinear activation function $f(\cdot)$ is applied to all the elements of the feature map arrays. A typical nonlinear activation function is the *ReLU* function as follows:

$$f(\cdot) = \max(u, 0) \tag{2}$$

Secondly, neighborhood values are merged into one representative value by applying pooling operation to the elements of feature mapping. Typical pooling operations are max-pooling and average-pooling. An average pooling operation is described as follows:

$$u_{ij} = \frac{1}{A^2}\sum_{a=1}^{A}\sum_{b=1}^{A} x_{i+a-1\ \ j+b-1} \tag{3}$$

where u_{ij} is the value of feature map after pooling operation, A is the height and width of pooling area, and x_{ij} is the value of a feature map after activation function.

Thirdly, all the values of feature maps are connected with the input nodes of the fully-connected layer after the pooling operation. The feedforward propagation process is shown as follows, and activation is also the *ReLU* function $f(\cdot)$, but an activation function of an output layer is a *Softmax* function:

$$x_j^l = f\left(\sum_{i=1}^{l} w_{ji}^l x_i^{l-1} + b_j^l\right) \tag{4}$$

$$y_k = e^{x_k} \Big/ \sum_{K=1}^{K} e^{x_k} \tag{5}$$

where x_j^l is the output value of the j_{th} node in the l_{th} layer after activation function, y_k is the output value of the k_{th} output node. K is the total number of output nodes, x_k is the input value of the k_{th} output node.

Lastly, a cost function C is needed to train a CNN model, and then the new weights $\boldsymbol{w}$ of a neural network are updated by subtracting the gradient of the cost function multiplied by a learning rate ε from the previous weights w,

$$C(\boldsymbol{w}) = -\frac{1}{N}\sum_{n=1}^{N}\sum_{k=1}^{K} d_{nk} \log_e y_{nk} \tag{6}$$

$$\boldsymbol{w}^{(t+1)} = \boldsymbol{w}^{(t)} - \varepsilon \nabla C = \boldsymbol{w}^{(t)} - \varepsilon \frac{\partial E}{\partial w} \tag{7}$$

where N is the total number of samples, K is the total number of output nodes , d_{nk} is the correct answer of the k_{th} output node in the n_{th} sample, and y_{nk} is the output value of the k_{th} output node in the n_{th} sample.

2.2 The diagnosis strategy

The fault diagnosis strategy for VRF system based on DCNN in this study mainly contains four part. Fig.1 is the fault diagnosis research strategy diagram in this study. The first part is experiments and data collection. We considered five types of common faults and their corresponding two and three simultaneous faults in VRF system. The second part is data preprocessing. For the proposed CNN model, this part only need the data preliminary processing step which only contains data integration and missing value elimination. The next part is FDD model training. The fault decoupling module is also effective at this time to provide construction variables to improve model performance. The end part is FDD model testing and fault diagnosis.

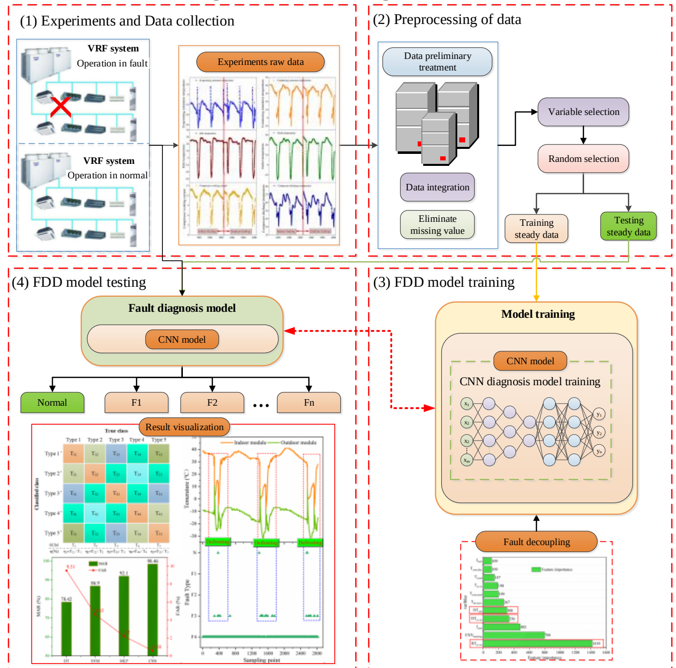

Fig. 1 The fault diagnosis research strategy diagram

3. EXPERIMENTAL SETUP AND DATA INTRODUCTION

A scheme of the experimental VRF system is shown in **Fig.2**. It is composed of five indoor units with independent temperature control and one outdoor unit. The rated cooling capacity of the five indoor units are 2.2kw, 2.8kw, 2.8kw, 3.6kw, and 7.1kw. The refrigerant of this VRF system is R410A with standard charge 6.3 kg. All experiments were performed in a standard psychrometric testing room, and all our operations are strictly in accordance with the following Chinese testing standards: GB/T 18837-2002, GB/T7725-2004 and GB/T 17758-2010. Five types of common faults in the VRF system is consider in this study: Indoor fouling(IF), outdoor fouling(OF), overcharge fault(OC), undercharge fault(UC), and indoor electronic expansion valve fault(EF).

The experimental data collection is carried out completely in accordance with the standard manual. The data collection time interval is 10s. After three month-long experiment, a total of 39051 pieces of experimental data were obtained under different working conditions.

The double simultaneous faults have the following combinations: IF+OF, OC+IF, OC+OF, UC+IF, UC+OF, EV+IF, EV+OF. The three simultaneous faults have the following combinations: OC+IF+OF50, OC+IF+OF75, UC+IF+OF50, UC+IF+OF75. Here, OF50 means that the indoor fouling fault intensity is 50%.

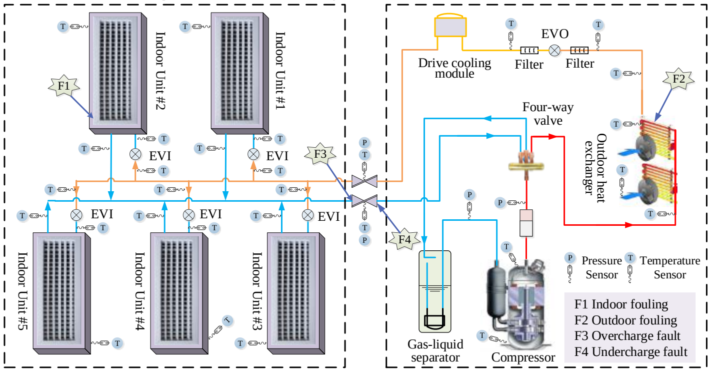

Fig.2. The schematic diagram of the VRF system

4. RESULT

4.1 Evaluation index

Let D denote a multi-label dataset, $|D|$ represents the total number of samples, L indicates the type of label, $|L|$ represents the total number of labels. H represents a multi-label classifier, let Z_i = H(x_i) be the prediction result set based on X_l with H.

Hamming loss represents the proportion of error samples in all labels, so the smaller the value, the stronger the classification ability of the network. Its calculation formula is as Eq. (8).

$$Hamming\ \ loss\ \ (H,D)=\frac{1}{D}\sum_{i=1}^{|D|}\frac{Y_i\Delta Z_i}{|L|} \tag{8}$$

Accuracy evaluates the proportion of correctly predicted examples over the whole data set. The accuracy is calculated as:

$$Accuracy\ \ (H,D)=\frac{1}{D}\sum_{i=1}^{|D|}\frac{Y_i\cap Z_i}{Y_i\cup Z_i} \tag{9}$$

The F1 score is a comprehensive criterion by taking account of both recall and precision. The expressions are demonstrated from Eq. (10) to Eq. (12)

$$Precision\ \ (H,D)=\frac{1}{D}\sum_{i=1}^{|D|}\frac{Y_i\cap Z_i}{|Z_i|} \tag{10}$$

$$Recall\ \ (H,D)=\frac{1}{D}\sum_{i=1}^{|D|}\frac{Y_i\cap Z_i}{|Y_i|} \tag{11}$$

$$\text{f1\_score}=\frac{2*Precision*Recall}{Precision+Recall} \tag{12}$$

The index of FAR is regularly used to evaluate the performance of the model's false alarm. It is defined as the ratio of the misjudge data to the total data in normal operation. The missed alarm rate (MAR) represents the proportion of the number of faults that the model misjudged the original fault data as normal to the total faults. The detailed calculation formula can be consulted in Literature[18].

4.2 Fault diagnosis

Table 1 shows the diagnosis results of the training set and testing set of the CNN model. The results show that the CNN model has excellent diagnostic performance for multi-connected systems when multiple faults and multiple simultaneous faults occur. Diagnosis accuracy reaches 98%. From the point of view of false alarm rate and missed alarm rate, the values are both lower than 2%. Among them, the missed alarm rate is lower, less than 0.5%. This shows that the CNN model has excellent fault recognition capabilities. Of course, from the perspective of recall and F1, the model still has room for improvement.

Table 1 The fault diagnosis results of CNN model

Evaluation index	Training data	Testing data
Accuracy	98.92%	98.28%
Hamming loss	0.23%	0.40%
Recall	85.98%	85.73%
F1_score	85.92%	85.59%
FAR	1.44%	1.65%
MAR	0.17%	0.38%

Fig.3 and Fig.4 are the CNN model fault diagnosis of online dataset. Among them, Fig.3 shows the diagnosis result under normal operation and double simultaneous faults. It can be seen from the timing diagram that when the VRF system is operating normally, the CNN model will still misjudge some data points as faults, such as OC, UC, IF, OF. But none of the cases was misjudged as EF fault. When the real operating state of the system is IF+OC fault, the CNN model judges three sampling points as normal and one sampling point as OC+OF fault. The case of model errors is much less than the data diagnosis during normal operation. This is also consistent with the performance of the model itself in the training set and test set.

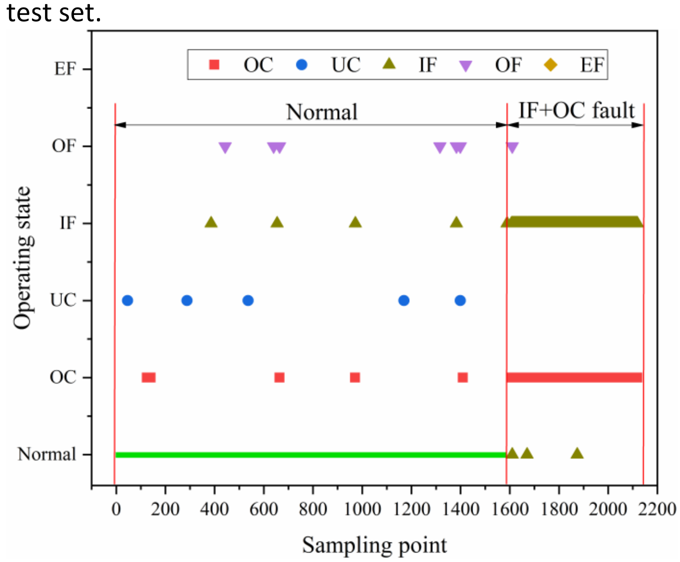

Fig.3. Timing diagram of online dataset (normal and double simultaneous faults)

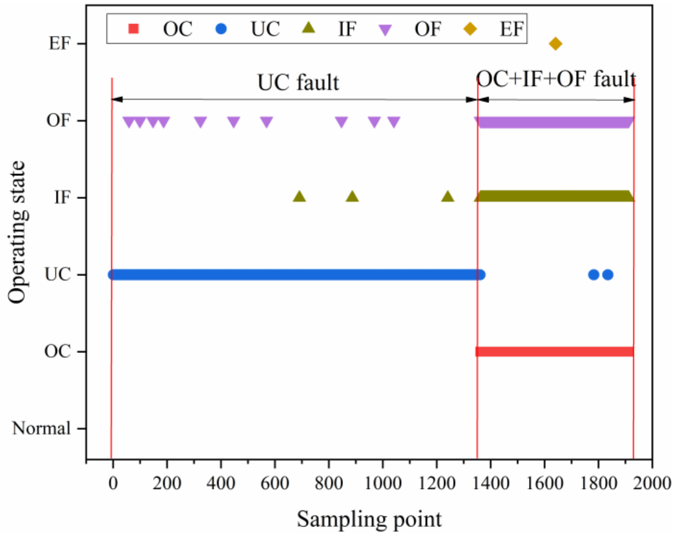

Fig.4. Timing diagram of online dataset (UC fault and three simultaneous faults)

Fig.4 shows the diagnosis result under UC fault operation and three simultaneous faults (OC+IF+OF) operation. The results show that the CNN model will have misjudgments between fault types. The CNN model misjudged the UC faults at 10 sample points as OF faults, and misjudges 3 sample points as IF faults. When three simultaneous faults occur, the CNN model shows excellent performance. Only at three sampling points, the actual "OC+IF+OF" fault is judged as simultaneous faults "UC+IF+OF" fault or "OF+EF" fault.

5. CONCLUTION

Aiming at the problem of simultaneous fault diagnosis of VRF systems, this paper obtains corresponding fault data through experiments, proposes a fault diagnosis method based on deep convolutional network, and uses online data sets to verify it. The results show that the method has a good ability to identify simultaneous faults in VRF systems, with a diagnosis accuracy of 98% and a Hamming loss value of 0.4%.

ACKNOWLEDGEMENT

The authors gratefully acknowledge the support of National Natural Science Foundation of China (Grant 51876070).

REFERENCE

[1] Y. Sun, F. Haghighat, B.C.M. Fung, A review of the-state-of-the-art in data-driven approaches for building energy prediction, Energy And Buildings, 221 (2020) 110022.
[2] J. Cho, Y. Kim, J. Koo, W. Park, Energy-cost analysis of HVAC system for office buildings: Development of a multiple prediction methodology for HVAC system cost estimation, Energy & Buildings, (2018) S0378778817341944.
[3] W. Wu, H.M. Skye, P.A. Domanski, Selecting HVAC systems to achieve comfortable and cost-effective residential net-zero energy buildings, Applied Energy, 212 (2018) 577-591.
[4] J.H. Wu, Z. Xu, F. Jiang, Analysis and development trends of Chinese energy efficiency standards for room air conditioners, Energy Policy, 125 (2019) 368-383.
[5] Y.B. Yu, D.C. Woradechjumroen, D.H. Yu, A review of fault detection and diagnosis methodologies on air-handling units, Energy And Buildings, 82 (2014) 550-562.
[6] Y. Zhao, F. Xiao, S.W. Wang, An intelligent chiller fault detection and diagnosis methodology using Bayesian belief network, Energy And Buildings, 57 (2013) 278-288.
[7] C. Fan, Y.C. Liu, X.Y. Liu, Y.J. Sun, J.Y. Wang, A study on semi-supervised learning in enhancing performance of AHU unseen fault detection with limited labeled data, Sustainable Cities And Society, 70 (2021).
[8] G.H. Zhang, H.S. Xiao, P.L. Zhang, B.L. Wang, X.T. Li, W.X. Shi, Y. Cao, Review on recent developments of variable refrigerant flow systems since 2015, Energy And Buildings, 198 (2019) 444-466.
[9] R. Yan, Z. Ma, G. Kokogiannakis, Y. Zhao, A sensor fault detection strategy for air handling units using cluster analysis, Automation In Construction, 70 (2016) 77-88.
[10] Y. Zhao, S. Wang, F. Xiao, Pattern recognition-based chillers fault detection method using Support Vector Data Description (SVDD), Applied Energy, 112 (2013) 1041-1048.
[11] S. Wang, Z. Jiang, Valve fault detection and diagnosis based on CMAC neural networks, Energy And Buildings, 36 (2004) 599-610.
[12] X. Zhu, Z. Du, Z. Chen, X. Jin, X. Huang, Hybrid model based refrigerant charge fault estimation for the data centre air conditioning system, International Journal of Refrigeration, 106 (2019) 392-406.
[13] G.N. Li, Y.P. Hu, H.X. Chen, J.Y. Wang, Y.B. Guo, J.Y. Liu, J. Li, Identification and isolation of outdoor fouling faults using only built-in sensors in variable refrigerant flow system: A data mining approach, Energy And Buildings, 146 (2017) 257-270.
[14] X. Zhao, M. Yang, H. Li, A virtual condenser fouling sensor for chillers, Energy And Buildings, 52 (2012) 68-76.
[15] Z. Zhou, G. Li, H. Chen, H. Zhong, Fault diagnosis method for building VRF system based on convolutional neural network: Considering system defrosting process and sensor fault coupling, Building And Environment, 195 (2021) 107775.
[16] B.J. Wu, W.J. Cai, H.R. Chen, X. Zhang, A hybrid data-driven simultaneous fault diagnosis model for air handling units, Energy And Buildings, 245 (2021).
[17] S. Asgari, R. Gupta, I.K. Puri, R. Zheng, A data-driven approach to simultaneous fault detection and diagnosis in data centers, Applied Soft Computing, 110 (2021) 107638.
[18] Z. Zhou, H. Chen, G. Li, H. Zhong, M. Zhang, J. Wu, Data-driven fault diagnosis for residential variable refrigerant flow system on imbalanced data environments, International Journal of Refrigeration, 125 (2021) 34-43.